



Design of Microstrip Composite Band Pass Filter for Ground Penetrating Radar

Yogantana Arum Panganti¹, Erfansyah Ali², A.A. Pramudita³

¹School of Electrical Engineering - Telkom University, Indonesia, yogantana@student.telkomuniversity.ac.id

²School of Electrical Engineering - Telkom University, Indonesia, erfansyahali@telkomuniversity.ac.id

³School of Electrical Engineering - Telkom University, Indonesia, pramuditaadya@telkomuniversity.ac.id

ABSTRACT

Ground Penetrating Radar (GPR) is a radar used to detect an object located/buried under the ground surface at a certain level of depth using electromagnetic radiation in the microwave band, without causing damage (non-destructive) on the surface. According to the function of the filter which can do frequency selection on a system, the need for a filter connected on the block next to the antenna in a GPR circuit is necessary. This filter helps the system to check and select the transmitted frequency and received frequency from the antenna. In this paper, microstrip structure is applied in filter design to obtain ultra-wideband (UWB) characteristic and to provide compact shape. The design of a two-patch case composite bandpass filter is proposed to fulfill the requirement. The design utilizes a combination of a stepped-impedance lowpass filter (LPF) as the upper stopband and quarter-wave highpass filter (HPF) to realize the lower stopband. A simulation is conducted on a dielectric substrate having a 4.4 dielectric constant and 1.6 mm thickness, followed by realization. The realization results show that the proposed filter have a good performance and produce 980 MHz wideband bandpass filter from 1.394-2.371 GHz with center frequency at 1.873 GHz. The filter has return loss value less than -10 dB and the filter rejection is sharp.

Keywords: Composite BPF, Microstrip filter, GPR, UWB.

1. INTRODUCTION

Underground object detection is one of the topics that continuously developed for use in various fields. Many activities require underground information effectively without damaging the ground/land, such as mining goods, underground cable maintenance, or underground pipe searching. Therefore, developed Ground Penetrating Radar (GPR), a technique that use electromagnetic wave to observe and detect an object at a certain location, certain depth, shape and conditions with non-destructive characteristic to avoid the damage on the surface with working frequency from 10 MHz until 10 GHz [1, 2]. The frequency range used in the GPR for

military field is 0.01 – 3 GHz [3]. GPR system consists of two main parts, namely transmitter, and receiver [4, 5]. GPR works by utilizing signal reflection from the object or surface. GPR has a transmitter antenna that connected with the transmitter block and filter, this antenna emits electromagnetic signals to the direction of the surface. When the electromagnetic signals hit an object, with different permittivity constant, apart of the signals are reflected and the other part is transmitted, this process continues until a certain depth [6, 7]. The reflected signals are captured by the receiver antenna, which then transmits the signals to the filter to be processed in the receiver block.

Filter is a tool that is used to filter out certain work frequency regions where only passing the desired frequency and detained the other frequencies [8]. With this filter, the system will not be disturbed by another frequency spectrum, so it can avoid interference with another channel. One of the filters that usually used in RADAR technology is Band Pass Filter (BPF). BPF greatly affects the system performance as a frequency selector that entering the system. The frequencies that meet the pass-band response will be transmitted whereas the frequency outside the passband will be muted. This BPF is lighter and simpler in terms of designing and does not require more space in its manufacture, making it easier to adjust to the conditions of the RADAR system [8].

Ultra-wideband (UWB) or wideband bandpass filter can be designed using a conventional method or by a direct cascade of a Low Pass Filter (LPF) and High Pass Filter (HPF). In the previous study [9], an arrangement of a three-line structure is introduced to increase the coupling, the filter presented has bandwidth still less than 70%. Then, in [10], a new formula for synthesizing microstrip bandpass filters with relatively wide bandwidth is introduced, the filter produced from this formula shows smaller bandwidth than the theoretical prediction.

Based on [11], several methods to construct a UWB bandpass filter are introduced, including the method to combine HPF and LPF. Both lower and upper stopband can be determined individually with the condition that both filters has matched

output and input impedance. Combined bandpass or composite bandpass reduces circuit area so entirely circuit can be greatly saved. The LPF is designed using a stepped-impedance structure because it is occupied less area and easier to design [12]. The HPF is designed using quarter-wave short-circuited stubs, where the stub is combined with the LPF high-impedance microstrip section [13]. The stub position of composite bandpass filter can be different. In the previous study [14], the paper comparing the design of the single and two-patch case composite filters, the result shows that composite Band Pass Filter with the two-patch case is show a filter with expected performance and a reaching bandwidth near 100%.

In this paper, a microstrip composite BP Fusing a two-patch case is designed and realized. The simulation of the filter is conducted on a dielectric substrate of FR-4 (epoxy) with 4.4 dielectric constant and 1.6 mm of thickness. The designed filter needs to fulfill the GPR specification which works in the range frequency of 1.3 GHz - 2.2 GHz according to existing GPR [15]. The GPR has return loss value less than -10 dB.

2. RESEARCH METHOD

The method used in this paper was concluded in three main procedures, namely the design and calculation of filter dimensions, simulation from the design and calculation, and the realization of the filter. The design has goals to achieve 900 MHz bandwidth from 1.3-2.2 GHz frequency range, less than -10 dB return loss value, and sharp rejection filter.

2.1 Microstrip Line

The structure of the microstrip consists of a single dielectric substrate between a ground plane and a conducting material. The conducting material has a width described as W and thickness described as t . The substrate has a thickness described as h and a relative dielectric constant described as ϵ_r , the bottom of the dielectric substrate is a ground plane [8].

The correct characteristic material for substrate and conducting material such as, dielectric constant, loss tangent, copper loss, and mechanical requirements are needed to overcome high return loss and low efficiency without changing the resonant frequency [16].

The width of the microstrip line can be calculated as given in [8]:

$$\frac{W}{h} \begin{cases} \frac{8e^A}{e^{2A}-1}, & \text{for } \frac{W}{h} < 2 \\ \frac{2}{\pi} \left[B - 1 - \ln(2B - 1) + \frac{\epsilon_r + 1}{2\epsilon_r} \left(\ln(B - 1) + 0.39 - \frac{0.61}{\epsilon_r} \right) \right], & \text{for } \frac{W}{h} \geq 2 \end{cases} \quad (1)$$

with,

$$A = \frac{Z_0}{60} \left\{ \frac{\epsilon_r + 1}{2} \right\}^{0.5} + \frac{\epsilon_r - 1}{\epsilon_r + 1} \left\{ 0.23 + \frac{0.11}{\epsilon_r} \right\} \quad (2)$$

$$B = \frac{60\pi^2}{Z_0 \sqrt{\epsilon_r}}$$

where, the substrate thickness is described as h and the substrate dielectric constant is described as ϵ_r .

The effective dielectric constant of the microstrip line is given approximately by [12],

$$\epsilon_{eff} = \frac{\epsilon_r + 1}{2} + \frac{\epsilon_r - 1}{2} \frac{1}{\sqrt{1 + \frac{12h}{W}}} \quad (3)$$

The guided wavelength of the quasi-TEM mode of microstrip is given by [12],

$$\lambda_g = \frac{300}{f(\text{GHz}) \sqrt{\epsilon_{eff}}} \text{ mm} \quad (4)$$

2.2 Composite BPF

The bandpass filter is designed using a composite method. This method used because it uses much less area than directly cascade LPF and HPF, it is also easy to realize for fabrication. Based on the research in [14], the BPF design in this paper used composite BPF with a two-patch case that can show good wide bandwidth up to 100%. The BPF consist of a low-Z and high-Z LPF, combined with quarter-wave short-circuited stub HPF. Figure 1 (a) shows the layout design of stepped-impedance LPF and Figure 1 (b) shows the proposed composite BPF.

2.3 Stepped Impedance LPF

Given in [12], the length of each line in stepped-impedance LPF can be determined as:

$$L_L = \tan^{-1} \left(\frac{\omega_c L}{Z_{hi}} \right) \frac{v_c}{\omega_c \sqrt{\epsilon_{hi,eff}}} \quad (5)$$

and

$$L_C = \sin^{-1} \left(\omega_c C Z_{low} \right) \frac{v_c}{\omega_c \sqrt{\epsilon_{low,eff}}} \quad (6)$$

where L_L and L_C are the length of microstrip transformed from the inductor and conductor respectively, L and C are the value of normalized element from the low-pass prototype, ω_c is the -3dB angular frequency, the speed of light in free space is described as v_c , and the effective dielectric constants $\epsilon_{hi,eff}$ is for the hi-Z and $\epsilon_{low,eff}$ is for low-Z microstrip sections.

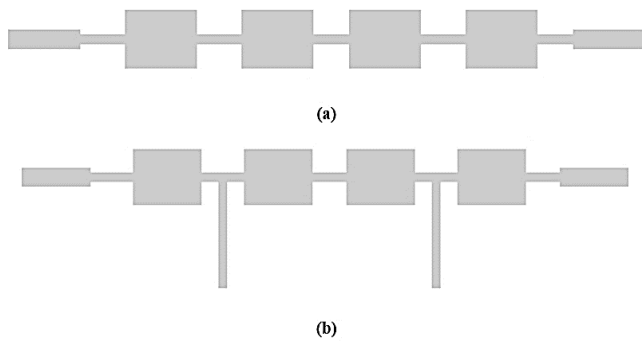


Figure 1: The layout of the filter (a) Stepped-impedance LPF (b) Composite BPF with a two-patch case.

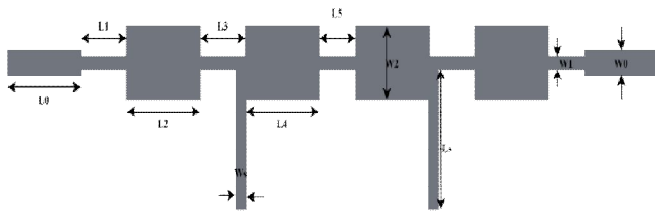


Figure 2: Geometry of composite BPF.

Table 1: Initial value of composite BPF dimensions.

Parameters	Value (mm)	Description
L1	8.56	Length of the line
L2	8.75	Length of the line
L3	13.045	Length of the line
L4	9.43	Length of the line
L5	13.32	Length of the line
Ls	33.8	Length of the stub
W1	0.32	Wide of the hi-Z section
W2	6.87	Wide of the low-Z section
Ws	0.32	Wide of the stub

2.4 Quarter-wave Short-circuited stub HPF

The length of each stub in HPF is quarter-wave short-circuit that given as [8]:

$$L_{stub} = \frac{\lambda_g}{4} \quad (7)$$

According to [14], the value of characteristic impedances has been selected as 130Ω and 30Ω respectively. Based on the calculation using (1-7) with respectively for LPF and HPF, the dimensions of composite BPF in Figure 2 can be seen in Table 1.

3. DESIGN OF COMPOSITE BPF

The simulation is performed to observe the filter characteristic and to analyze the parameter of the filter based on the calculation in (1-7). The simulation of stepped-impedance

LPF with initial dimension in Figure 3 is conducted. The result from the simulation is still not as expected, because there are frequency shifting in the working frequency.

In Figure 4 (a) the cut-off frequency is noted at 2.1 GHz instead of the initial specification at 2.2 GHz. Excluding the frequency shifting, the LPF has good shape and sharp rejection after the cut-off frequency. The return loss value is varying with the maximum at -12 dB, but in 2.02-2.1 GHz the return loss value reached -10 until -3 dB as shown in Figure 4 (b). The stepped-impedance LPF has relatively good performance except the frequency shifting. With those results, the stepped-impedance LPF is not optimized.

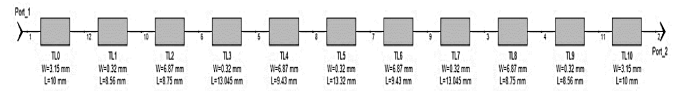


Figure 3: Initial design of stepped-impedance LPF.

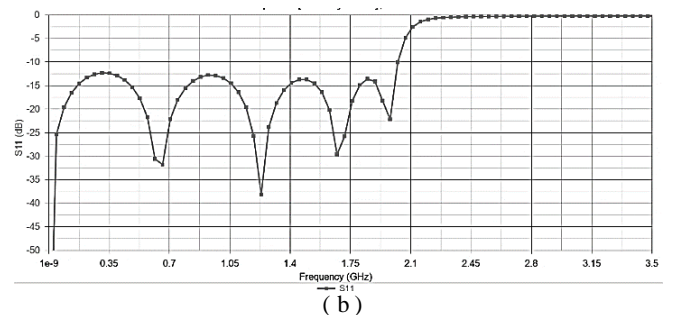
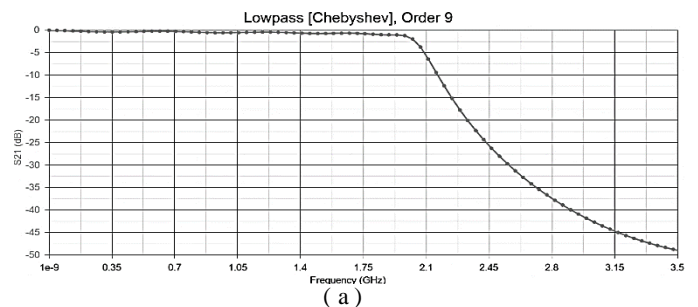


Figure 4: Stepped-impedance LPF simulation. (a) Insertion loss result. (b) Return loss result.

The quarter-wave short-circuited HPF combined with the stepped-impedance LPF. The HPF stubs tapped at the high impedance of LPF using a two-patch case. The geometry of the new combined filter can be seen in Figure 2. HPF is realizing the lower stopband at 1.3 GHz frequency cut-off which makes the LPF with 2.2 GHz frequency cut-off act as the upper stopband and the filter become BPF after tapped. The initial design of the new combined filter can be seen in Figure 5 along with its dimensions value.

The simulation in Figure 6 shows a BPF with -3dB bandwidth around 1400 MHz from a lower cut-off frequency at 525 MHz until the upper cut-off frequency at 1925 MHz with a center frequency of 1225 MHz. The Insertion Loss (IL) at the center

frequency is -0.78 dB, meanwhile, IL at the upper cut-off frequency (f_{cu}) and lower cut-off frequency (f_{cl}) is -3.9 dB. The working frequency is shifting when compared with the specification and the bandwidth is wider than the needed specification. The return loss result of the simulation is less than -10 dB, it has indicated that the filter works relatively well, but the bandwidth and frequency range does not match with the specifications needed. Therefore, dimension optimization is necessary to improve and fix the filter performance.

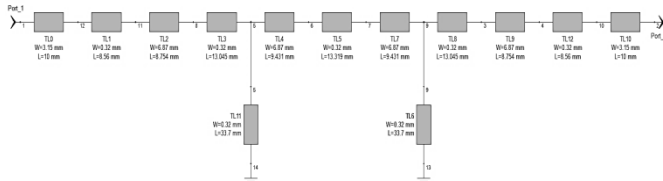


Figure 5: Initial design of composite BPF.

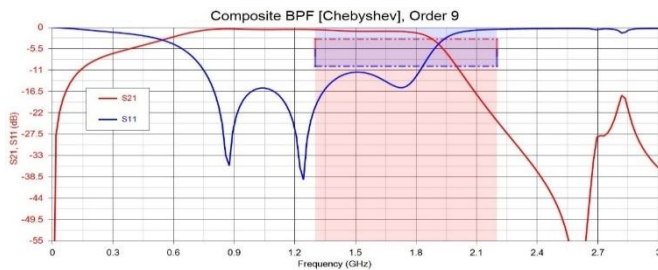


Figure 6: Composite BPF simulation result.

The optimization is done by changing the filter dimension using trial-error method (parameter sweep) and optimal design ability owing by ADS software (Genesys) until the filter characteristic matches the needed specifications. The dimension change is performed sequentially from the microstrip wide until the microstrip length. After optimization of each parameter, the most appropriate dimension of the filter is simulated. The parameter after the final optimization can be seen in Table 2 along with the comparison with the initial parameter.

Based on Figure 7, the bandwidth obtained after the optimization is around 900 MHz with working frequencies range from 1300 MHz to 2200 MHz. The bandwidth and frequency range are meet with the specifications.

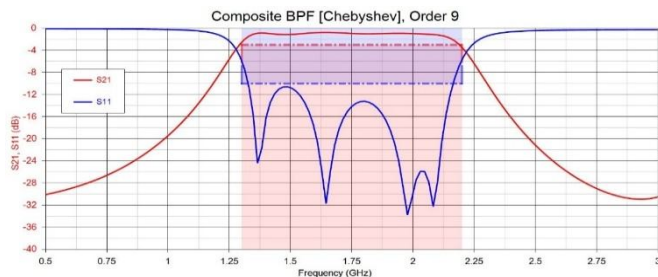


Figure 7: The simulation of composite BPF after optimization.

Table 2: Comparison of composite BPF dimensions.

Parameters	Initial Value (mm)	Optimization Value (mm)
L1	8.56	12.3
L2	8.75	4.5
L3	13.045	14.7
L4	9.43	11.8
L5	13.32	14.7
Ls	33.8	11
W1	0.32	0.15
W2	6.87	6.5
Ws	0.32	2.5

Table 3: Final value of composite BPF dimensions.

Parameters	Final Value (mm)	Description
L1	12.3	Length of the line
L2	4.5	Length of the line
L3	14.7	Length of the line
L4	11.8	Length of the line
L5	14.7	Length of the line
Ls	11	Length of the stub
W1	0.15	Wide of the hi-Z section
W2	6.5	Wide of the low-Z section
Ws	2.5	Wide of the stub

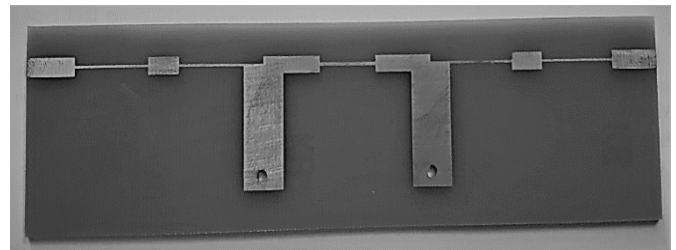


Figure 8: Realization of composite BPF.

The Insertion Loss (IL) at the center frequency is -0.97 dB, meanwhile, IL at the upper and lower cut-off frequency is -4 dB. The return loss value generated from -34 dB with a maximum in -10 dB, which shows that the filter has good performance. The optimization improves the filter performance and fixes the filter until it reaches the needed specifications. The final values of composite BPF are shown in Table 3. The realization of the filter is shown in Figure 8.

4. MEASUREMENT AND ANALYSIS

In this filter, the measured parameters are insertion loss (IL), return loss, and bandwidth. Insertion loss and return loss describe the absorbed power and loss power of the filter. Those two are related to the filter port using an SMA connector. According to Figure 9, the bandwidth results in the simulation is 900 MHz with center frequency at 1300 MHz and the bandwidth results in the measurement is 980 MHz with center frequency at 1873 MHz. There is a working frequency difference of 100 MHz.

The insertion loss value of the simulation result is -0.97 dB at the center frequency and -4 dB at the upper and lower cut-off frequency. Meanwhile, the insertion loss value of the measurement result is -2.025 dB at the center frequency and the upper and lower cut-off frequency are -5.068 dB and -5.144 dB respectively. The comparison of return loss results is shown in Figure 10. The return loss value of the simulation result is ranging from -34 dB until -10 dB. Meanwhile, the return loss value of the measurement result is ranging from -38.2 dB with a maximum at -10 dB.

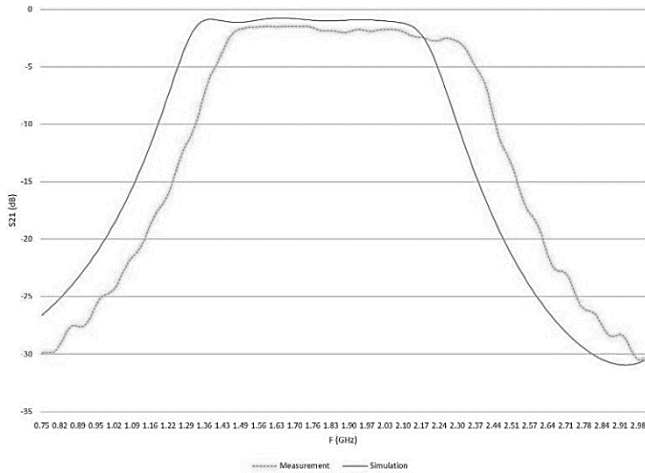


Figure 9: The Comparison result between simulation and fabrication (realization) measurement of insertion loss.

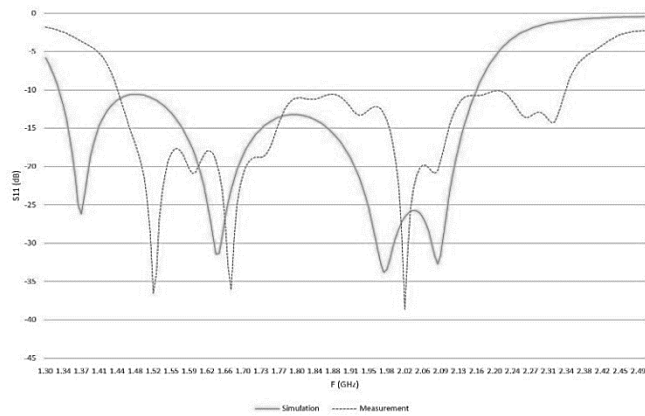


Figure 10: The Comparison result between simulation and fabrication (realization) measurement of return loss.

From the obtained data, there is a difference in the value of insertion loss and return loss. The simulation shows that the insertion loss is higher which means that the simulation is obtained more power than the measurement. The return loss of both simulation and measurement is relatively the same, the difference is the measurement has more ripple due to the cable. That problem likely emerges due to the connector type and connector soldering factor which can result in loss and mismatch. In the simulation, the end-tip of the microstrip tap is connected to the connector port. Meanwhile, the realization connected the connector with half-length of microstrip tap. Improper placement of connector can cause different insertion loss and return loss, so the connector must be placed and soldered right in the middle of microstrip tap wide.

The specification for the bandwidth is 900 MHz meanwhile the specification for the working frequency is 1300-2200 MHz. The result of the simulation shows the same result with the specifications. Meanwhile, the result of measurement shows that the bandwidth is 980 MHz and the working frequency is 1394-2371 MHz. That result shows that the working frequency is shifting, and the bandwidth is wider than the specification and simulation.

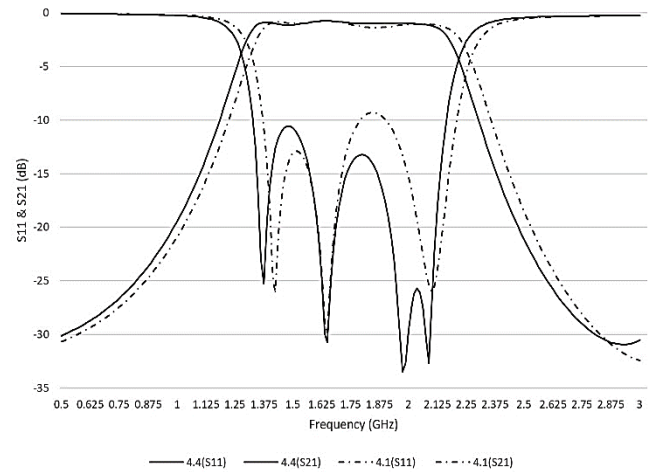


Figure 11: Comparison of substrate permittivity.

The frequency shifting and wider bandwidth are estimated due to the fabrication dimension. The machine for fabrication has maximum precision around 0.1-0.2 mm whereas the simulation filter dimension has high precision until 2-3 number behind the commas. The dimensional changes may result in different work frequencies and the wide of the bandwidth. The material used also influences the fabrication. In the simulation, the substrate is using FR-4 (epoxy) with 1.6 mm of thickness, 4.4 dielectric constant, and the conductor is using copper with a thickness of 0.035 mm. Whereas that occurs when realized is the substrate using FR-4 with permittivity around 4.1-4.6.

According to the simulation conducted, the permittivity of the substrate affects the work frequency. The smaller the permittivity then the work frequency is shifting to the bigger axis. Based on simulation illustrated in Figure 11, the substrate used in the realization have permittivity of 4.1 as described from [17].

5. CONCLUSION

In this paper, the processes of design, simulation, and realization of composite microstrip bandpass filter for GPR has completed. The usage of a two-patch case in the composite BPF is recommended to achieve wider bandwidth up to 100%. The filter resulting the working frequency of the realization is 1.394-2.371 GHz with center frequency at 1.873 GHz. Meanwhile, the working frequency needed in the specification is 1.3-2.2 GHz with center frequency at 1.75 GHz. Those results can be concluded that the working frequency is shifting due to the dimension changing in the fabrication process.

The bandwidth of the realized filter is 980 MHz, 80 MHz wider than the needed specification which should only have a bandwidth of 900 MHz. That problem is due to the fabrication that has less precision or due to the difference of material specification used for realization. The result of the return loss is ranging but not surpass -10 dB, meaning the filter has small reflected power which shows that the filter has good performance. The measurement result also shows the value of insertion loss is smaller than the needed specification. That problem is due to the connector type and connector soldering factor which can result in loss and mismatch.

REFERENCES

- [1] D. J. Daniels. **Ground Penetrating Radar - 2nd Edition**, London, United Kingdom: The Institution of Engineering and Technology, 2004.
- [2] J. Ali, N. Abdullah, M. Y. Ismail, E. Mohd and S. M. Shah. **Ultra-Wideband Antenna Design for GPR Application: A Review**, *International Journal of Advanced Computer Science and Applications*, vol. 8, 2017.
- [3] Hertl, I., & Strýček, M. **UWB Antennas for Ground Penetrating Radar Application**. *19th International Conference on Applied Electromagnetics and Communications*, pp. 1-4, 2007.
- [4] Skolnik, M. I. **Introduction to Radar Systems**. The McGraw-Hill Companies, 2008.
- [5] J. Ali, N. Abdullah, R. Yahya, A. Joret, and E. Mohd. **Ultra-Wideband Antenna with Monostatic/Bistatic Configurations for Search & Rescue Applications**, *International Journal of Advanced Trends in Computer Science and Engineering*, vol. 8, pp. 219-223, 2019.
- [6] Annan, A. **Electromagnetic Principles of Ground Penetrating Radar**, In *Ground Penetrating Radar Theory and Applications*, H. M. JOL, Ed. Slovenia: Elsevier B.V, 2009, pp. 3-37.
- [7] Ghazali, Rosmadi et al. **Estimation of Different Subsurface Materials Depth Using Ground Penetrating Radar**. *International Journal of Advanced Trends in Computer Science and Engineering*, vol 8, no. 1.3, pp. 363-370, 2019.
- [8] Hong, J.-S., & Lancaster, M. J. **Microstrip Filters for RF/Microwave Applications**. New York: John Wiley & Sons, Inc, 2001.
- [9] Kuo, J.-T., & Shih, E. **Wideband bandpass filter design with three-line microstrip structures**, in *IEE Proceedings - Microwaves, Antennas and Propagation*, vol. 149, no. 56, 2002, pp. 243-247.
- [10] Chin, K.-S., Lin, L.-Y., & Kuo, J.-T. **New formulas for synthesizing microstrip bandpass filters with relatively wide bandwidths**. *IEEE Microwave and Wireless Components Letters*, vol. 15, no. 5, pp. 231 - 233, 2004.
- [11] Kumar, M., & Kumar, D. S. **Different Methods of Designing Ultra Wideband Filters in Various Applications-A Review**. *International Journal of R&D in Engineering, Science and Management*, vol. 1, no. I, pp. 1-7, 2014.
- [12] Pozar, D. M. **Microwave Engineering - 2nd Edition**, New York: John Wiley & Sons, Inc, 1998.
- [13] Seghier, S., Benabdallah, N., Benahmed, N., & Nouri, K. **Design and Optimization of a Microstrip Bandpass Filter for Ultra Wideband (UWB) Wireless Communication**. *International Journal of Information and Electronics Engineering*, vol. 6, no.4, pp. 230-233, 2016.
- [14] Hsu, C.-L., Hsu, F.-C., & Kuo, J.-K. (2005). **Microstrip bandpass filters for Ultra-Wideband (UWB) wireless communications**, in *IEEE MTT-S International Microwave Symposium Digest* Long Beach, CA, USA, 2005, pp. 679-682.
- [15] MAL°A MIRA 16 Ground Penetrating Radar, GUIDELINEGEO, datasheet.
- [16] Pandimadevi, M. et al. **Design Issues of Flexible Antenna -A Review**, *International Journal Of Advanced Trends In Computer Science And Engineering*, vol 8, no. 4, pp. 1386-1394, 2019.
- [17] Positive Presensitized Copper Clad Boards 600 Series, MG Chemicals, technical Data Sheet